

Ultraviolet Photodissociation at 355 nm of Fluorescently Labeled Oligosaccharides

Jeffrey J. Wilson and Jennifer S. Brodbelt*

Department of Chemistry and Biochemistry, 1 University Station A5300, University of Texas at Austin, Austin, Texas 78712

Ultraviolet photodissociation (UVPD) produces complementary fragmentation to collision-induced dissociation (CID) when implemented for activation of fluorescently labeled oligosaccharide and glycan ions. Reductive amination of oligosaccharides with fluorophore reagents results in efficient photon absorption at 355 nm, producing fragment ions from the nonreducing end that do not contain the appended fluorophore. In contrast to the fragment ions observed upon UVPD (A- and C-type ions), CID produces mainly reducing end fragments retaining the fluorophore (Y-type ions). UVPD affords better isomeric differentiation of both the lacto-N-fucopentaoses series and the lacto-N-difucosylhexaoses series, but in general, the combination of UVPD and CID offers the most diagnostic elucidation of complex branched oligosaccharides. Four fluorophores yielded similar MS/MS results; however, 6-aminoquinoline (6-AQ), 2-amino-9(10H)-acridone (AMAC) and 7-aminomethylcoumarin (AMC) afforded more efficient photon absorption and subsequent dissociation than 2-aminobenzamide (2-AB). UVPD also was useful for characterization of glycans released from ribonuclease B and derivatized with 6-AQ. Lastly, electron photodetachment dissociation of oligosaccharides derivatized with 7-amino-1,3-naphthalenedisulfonic acid (AGA) yielded unique cross-ring cleavages similar to those obtained by electron detachment dissociation.

Glycomics has become a research field of great interest as it provides a window into understanding an assortment of cellular functions related to health and disease.¹ Oligosaccharides as well as glycans (oligosaccharides released from glycoproteins) participate in a variety of cell processes such as cellular signaling and differentiation, virus infection and replication, immune response, and inflammation in addition to regulation of biochemical pathways.^{2–9} Furthermore, glycosylation is now recognized as the most common posttranslational modification of eukaryotic proteins in which greater than 50% of these proteins can undergo glycosylation.¹⁰

Glycans are particularly challenging to study due to their structural diversity stemming from the various nonlinear branching structures as well as their array of intersaccharide linkages. Moreover, the position of their attachment within the protein structure as well as the type of glycosylation, N- or O-linked, is essential for comprehensive mapping of glycoproteins. N-Glycosylation solely occurs through the creation of an N-glycosidic bond with Asn where the N-linked amino acid position sequence follows Asn-X-Ser/Thr (where X cannot be Pro), whereas O-glycosylation occurs via Ser or Thr residues in proteins. These modifications can reside not only at multiple locations throughout the proteins but also with a variety of different glycan forms attached to each individual site. The rigorous identification of these complex glycan structures typically requires several analytical techniques such as MS, NMR, endo- and exoglycosidase digestions, liquid chromatography, and monosaccharide analysis used collectively for complete characterization.^{11,12}

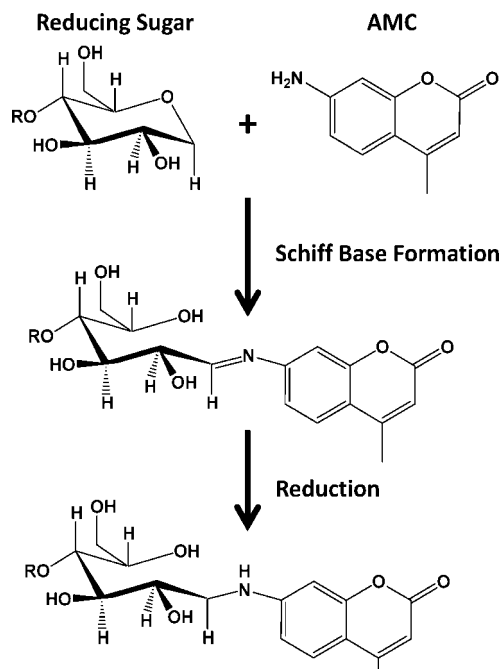
Fluorescent labeling of oligosaccharides is frequently employed for the enhancement of the detection sensitivity as well as improvement of separation in HPLC and fluorophore-assisted capillary electrophoresis (FACE) analysis.^{13,14} An assortment of fluorophores have been evaluated with no universal reagent yet providing unsurpassed results for all types of oligosaccharide analysis.¹⁴ Charged fluorophores are typically employed for FACE analysis in which the charged character facilitates separation. On the other hand, the hydrophilic nature of neutral and acidic oligosaccharides makes their separation difficult by HPLC; therefore, hydrophobic fluorophores are desired for improving separation characteristics.¹⁴ Additionally, fluorophores differ in both their spectroscopic properties and reaction yields, which further influences their suitability for particular analytical objectives.¹⁴ The most common method for appending a fluorophore to an oligosaccharide has been via reductive amination through the reducing end sugar via a Schiff base intermediate.¹⁵ These commonly used derivatization strategies also make them a natural approach for implementation of ultraviolet photodis-

* To whom correspondence should be addressed. E-mail: jbrodbelt@mail.utexas.edu.

- (1) Ohtsubo, K.; Marth, J. D. *Cell (Cambridge, Mass.)* **2006**, *126*, 855–867.
- (2) Vigerust, D. J.; Shepherd, V. L. *Trends Microbiol.* **2007**, *15*, 211–218.
- (3) Kojima, K. *Trends Glycosci. Glycotechnol.* **1998**, *10*, 415–416.
- (4) Kitajima, K. *Jikken Igaku* **2007**, *25*, 1079–1087.
- (5) Helenius, A.; Aebi, M. *Annu. Rev. Biochem.* **2004**, *73*, 1019–1049.
- (6) Bin, S.; Zhou, A.; Cheng, P. *Zhongguo Shouyi Xuebao* **2006**, *26*, 344–346.
- (7) Helenius, A.; Aebi, M. *Science (Washington, DC)* **2001**, *291*, 2364–2369.

- (8) Kukuruzinska, M. A.; Lennon, K. *Crit. Rev. Oral Biol. Med.* **1998**, *9*, 415–448.
- (9) Fannon, M.; Forsten, K. E.; Nugent, M. A. *Biochemistry* **2000**, *39*, 1434–1445.
- (10) Van den Steen, P.; Rudd, P. M.; Dwek, R. A.; Opdenakker, G. *Crit. Rev. Biochem. Mol. Biol.* **1998**, *33*, 151–208.
- (11) Morelle, W.; Michalski, J.-C. *Nat. Protoc.* **2007**, *2*, 1585–1602.
- (12) Geyer, H.; Geyer, R. *Biochim. Biophys. Acta, Proteins Proteomics* **2006**, *1764*, 1853–1869.
- (13) Anumula, K. R. *Anal. Biochem.* **2006**, *350*, 1–23.
- (14) Shilova, N. V.; Bovin, N. V. *Russ. J. Bioorg. Chem.* **2003**, *29*, 309–324.
- (15) Prime, S. B.; Shipston, N. F.; Merry, T. H. *BioMethods (Basel)* **1997**, *9*, 235–260.

Scheme 1. Reductive Amination Reaction Involving a Reducing End Sugar and Fluorescent Label AMC^a



^a The reaction forms a Schiff base intermediate, which undergoes reduction to yield a stable linkage between the fluorophore and oligosaccharide structure.

sociation (UVPD) mass spectrometry for structural characterization of oligosaccharides in which the attached chromophores enhance UV absorptivity for ion activation, as illustrated in the present study.

In general, tandem mass spectrometry has proven to be a powerful tool for the structural analysis of biomolecules, especially in proteomics and genomics,^{16–18} and also for the identification of glycans.^{19,20} For example, collision-induced dissociation (CID), the most widely used activation method, principally results in the formation of diagnostic B-/Y- and C-/Z-type fragment ions for unmodified oligosaccharides (using the Domon and Costello nomenclature as illustrated in Scheme 2).^{21,22} Other activation methods, including postsource decay,^{23,24} electron capture dissociation,^{25–27} electron detachment dissociation (EDD),^{28,29} electron-transfer dissociation,^{30,31} infrared multiphoton dissociation (IRMPD),^{32–36} and more recently UVPD^{37,38} at 157 nm, have all

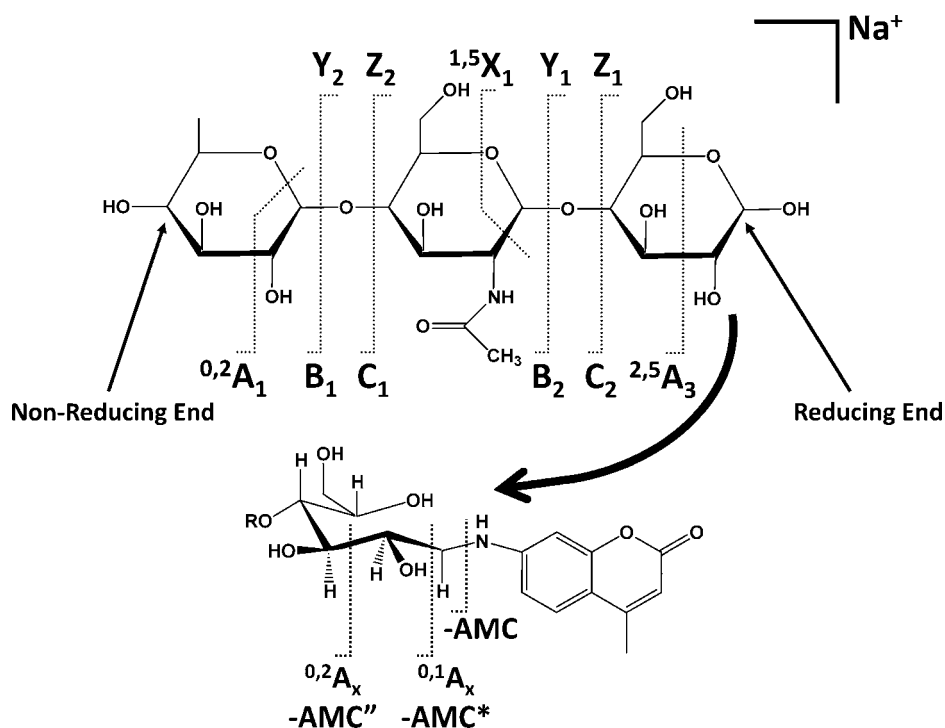
been employed for the structural determination of oligosaccharides, glycans, and glycopeptides. The latter photodissociation (PD) methods have predominantly used in FTICR and quadrupole ion trap (QIT) mass spectrometers. Photodissociation provides several distinct advantages over traditional CID in QIT mass spectrometers. Ion activation by photodissociation is independent of the trapping rf voltage, thus allowing efficient retention of fragment ions over a broad m/z range. Moreover, the nonresonant nature of PD results in the activation of all ions, not just the selected precursor, which causes informative secondary dissociation and bypasses the need for complex MSⁿ scan functions. These advantages of QITs have been exploited in the analysis of an array of biomolecules ranging from oligosaccharides^{35,37} and DNA,^{39–43} to peptides and proteins.^{44–58}

There have been several previous studies that utilized PD specifically for the characterization of oligosaccharides. Lancaster et al. reported that N-linked oligosaccharides readily undergo cross-ring cleavages upon IRMPD, but not by CID, in an FTICR

(16) Wysocki Vicki, H.; Resing Katheryn, A.; Zhang, Q.; Cheng, G. *Methods* **2005**, *35*, 211–222.
 (17) Cantor, C. R.; Broude, N.; Sano, T.; Przetakiewicz, M.; Smith, C. L. *Mass Spectrom. Biol. Sci.* **1996**, 519–533.
 (18) Tost, J.; Gut, I. G. *Mass Spectrom. Rev.* **2002**, *21*, 388–418.
 (19) Wuhler, M.; Catalina, M. I.; Deelder, A. M.; Hokke, C. H. *J. Chromatogr., B: Anal. Technol. Biomed. Life Sci.* **2007**, *849*, 115–128.
 (20) Morelle, W.; Canis, K.; Chirat, F.; Faid, V.; Michalski, J.-C. *Proteomics* **2006**, *6*, 3993–4015.
 (21) Domon, B.; Costello, C. E. *Glycoconjugate J.* **1988**, *5*, 397–409.
 (22) Harvey, D. J.; Bateman, R. H.; Green, M. R. *J. Mass Spectrom.* **1997**, *32*, 167–187.
 (23) Zaia, J. *Mass Spectrom. Rev.* **2004**, *23*, 161–227.
 (24) Harvey, D. J. *Mass Spectrom. Rev.* **1999**, *18*, 349–450.
 (25) Hakansson, K.; Chalmers Michael, J.; Quinn John, P.; McFarland Melinda, A.; Hendrickson Christopher, L.; Marshall Alan, G. *Anal. Chem.* **2003**, *75*, 3256–3262.
 (26) Mirgorodskaya, E.; Roepstorff, P.; Zubarev, R. A. *Anal. Chem.* **1999**, *71*, 4431–4436.
 (27) Adamson, J. T.; Hkansson, K. *Anal. Chem. (Washington, DC)* **2007**, *79*, 2901–2910.

(28) Wolff, J. J.; Amster, I. J.; Chi, L.; Linhardt, R. J. *J. Am. Soc. Mass Spectrom.* **2007**, *18*, 234–244.
 (29) Adamson, J. T.; Hakansson, K. J. *Am. Soc. Mass Spectrom.* **2007**, *18*, 2162–2172.
 (30) Zhang, Q.; Frollov, A.; Tang, N.; Hoffmann, R.; van de Goor, T.; Metz, T. O.; Smith, R. D. *Rapid Commun. Mass Spectrom.* **2007**, *21*, 661–666.
 (31) Hogan, J. M.; Pitteri, S. J.; Chrisman, P. A.; McLuckey, S. A. *J. Proteome Res.* **2005**, *4*, 628–632.
 (32) Park, Y.; Lebrilla, C. B. *Mass Spectrom. Rev.* **2005**, *24*, 232–264.
 (33) Xie, Y.; Lebrilla, C. B. *Anal. Chem.* **2003**, *75*, 1590–1598.
 (34) Lancaster, K. S.; An, H. J.; Li, B.; Lebrilla, C. B. *Anal. Chem.* **2006**, *78*, 4990–4997.
 (35) Pikulski, M.; Hargrove, A.; Shabbir, S. H.; Anslyn, E. V.; Brodbelt, J. S. *J. Am. Soc. Mass Spectrom.* **2007**, *18*, 2094–2106.
 (36) Fukui, K.; Takada, Y.; Sumiyoshi, T.; Imai, T.; Takahashi, K. *J. Phys. Chem. B* **2006**, *110*, 16111–16116.
 (37) Devakumar, A.; Mechref, Y.; Kang, P.; Novotny, M. V.; Reilly, J. P. *Rapid Commun. Mass Spectrom.* **2007**, *21*, 1452–1460.
 (38) Devakumar, A.; Thompson, M. S.; Reilly, J. P. *Rapid Commun. Mass Spectrom.* **2005**, *19*, 2313–2320.
 (39) Keller, K. M.; Brodbelt, J. S. *Anal. Biochem.* **2004**, *326*, 200–210.
 (40) Wilson, J. J.; Brodbelt, J. S. *Anal. Chem.* **2007**, *79*, 2067–2077.
 (41) Gabelica, V.; Rosu, F.; De Pauw, E.; Antoine, R.; Tabarin, T.; Broyer, M.; Dugourd, P. *J. Am. Soc. Mass Spectrom.* **2007**, *18*, 1990–2000.
 (42) Gabelica, V.; Rosu, F.; Tabarin, T.; Kinet, C.; Antoine, R.; Broyer, M.; De Pauw, E.; Dugourd, P. *J. Am. Chem. Soc.* **2007**, *129*, 4706–4713.
 (43) Gabelica, V.; Tabarin, T.; Antoine, R.; Rosu, F.; Compagnon, L.; Broyer, M.; De Pauw, E.; Dugourd, P. *Anal. Chem.* **2006**, *78*, 6564–6572.
 (44) Antoine, R.; Joly, L.; Tabarin, T.; Broyer, M.; Dugourd, P.; Lemoine, J. *Rapid Commun. Mass Spectrom.* **2007**, *21*, 265–268.
 (45) Ly, T.; Julian, R. R. *J. Am. Chem. Soc.* **2008**, *130*, 351–358.
 (46) Joly, L.; Antoine, R.; Allouche, A.-R.; Broyer, M.; Lemoine, J.; Dugourd, P. *J. Am. Chem. Soc.* **2007**, *129*, 8428–8429.
 (47) Fung, Y. M. E.; Kjeldsen, F.; Silivra, O. A.; Chan, T. W. D.; Zubarev, R. A. *Angew. Chem., Int. Ed.* **2005**, *44*, 6399–6403.
 (48) Payne, A. H.; Glish, G. L. *Anal. Chem.* **2001**, *73*, 3542–3548.
 (49) Tabarin, T.; Antoine, R.; Broyer, M.; Dugourd, P. *Rapid Commun. Mass Spectrom.* **2005**, *19*, 2883–2892.
 (50) Crowe, M. C.; Brodbelt, J. S. *Anal. Chem.* **2005**, *77*, 5726–5734.
 (51) Drader, J. J.; Hannis, J. C.; Hofstadler, S. A. *Anal. Chem.* **2003**, *75*, 3669–3674.
 (52) Hashimoto, Y.; Hasegawa, H.; Yoshinari, K.; Waki, I. *Anal. Chem.* **2003**, *75*, 420–425.
 (53) Yoon, T. O.; Choi, C. M.; Kim, H. J.; Kim, N. J. *Bull. Korean Chem. Soc.* **2007**, *28*, 619–623.
 (54) Wilson, J. J.; Brodbelt, J. S. *Anal. Chem.* **2006**, *78*, 6855–6862.
 (55) Wilson, J. J.; Brodbelt, J. S. *Anal. Chem. (Washington, DC)* **2007**, *79*, 7883–7892.
 (56) Wilson, J. J.; Brodbelt, J. S. *J. Am. Soc. Mass Spectrom.* **2008**, *19*, 257–260.
 (57) Kim, T.-Y.; Thompson Matthew, S.; Reilly James, P. *Rapid Commun. Mass Spectrom.* **2005**, *19*, 1657–1665.
 (58) Thompson, M. S.; Cui, W.; Reilly, J. P. *J. Am. Soc. Mass Spectrom.* **2007**, *18*, 1439–1452.

Scheme 2. Oligosaccharide Fragmentation Nomenclature Adapted from Domon and Costello Nomenclature^a



^a The bottom scheme shows the $-AMC^*$ and $-AMC''$ nomenclature used to represent the resulting $^{0,1}A_x$ and $^{0,2}A_x$ product ions, respectively.

mass spectrometer.³⁴ Xie et al. noted that the varying IRMPD dissociation thresholds of alkali metal cationized oligosaccharides enhanced isomer differentiation.³³ An IR wavelength-tunable free electron laser for infrared experiments was used by Fukui et al. to investigate the optimal dissociation wavelengths of sodium-cationized oligosaccharides.³⁶ Pikulski et al. reported that oligosaccharides derivatized with an IR-chromogenic boronic acid underwent efficient IRMPD and extensive secondary dissociation in a QIT, producing fragment ions that result via cleavage from only the nonreducing ends.³⁵ In terms of UVPD of oligosaccharides, Devakumar et al. reported two studies utilizing an excimer laser at $\lambda = 157$ nm.^{37,38} UVPD at 157 nm induced extensive crossring cleavages, which provided key information about saccharide linkage positions.

In this study, we report the merits and challenges associated with the application of UVPD at 355 nm to fluorescently labeled oligosaccharides in a QIT mass spectrometer. While CID produces fragment ions retaining the fluorophore attached through the reducing end sugar, UVPD provides complementary information for these complex structures via the formation of fragment ions without the fluorophore and instead emphasizing the nonreducing end of the oligosaccharide. UVPD affords streamlined isomeric differentiation of various oligosaccharide branching structures. Electron photodetachment dissociation (EPD) experiments are also conducted on oligosaccharides modified with an acidic fluorophore reagent to induce radical type cleavages.

EXPERIMENTAL SECTION

Reagents. All chemicals were purchased from Sigma Aldrich (St. Louis, MO) except the following: 6-aminoquinoline (6-AQ) and 2-aminobenzamide (2-AB) were obtained from Acros Organ-

ics; 7-amino-4-methylcoumarin (AMC) from MP Biomedicals, Inc. (Irvine, CA); and 2-amino-9(10*H*)acridone (AMAC) and 7-aminonaphthalene-1,3-disulfonic acid (AGA) from AnaSpec (San Jose, CA). These fluorescent reagents are displayed in Figure 1. All oligosaccharides were purchased from V-Laboratories (Covington, LA) except lacto-*N*-difucohexaose (LNDFH)-Ib, which was purchased from Sigma Aldrich. The lacto-*N*-fucopentaose (LNFP) and LNDFH oligosaccharide series are displayed in Figure 2. Glycerol free peptide *N*-glycosidase F (PNGase F) was purchased from New England Biolabs (Ipswich, MA).

Deglycosylation. Enzymatic treatment of glycoproteins was conducted following the manufacturer's protocol. In short, 20 μ g of a glycoprotein solution was diluted into 10 μ L of 0.5% sodium dodecyl sulfate and 0.04 M dithiothreitol solution and then heated to 100 °C for 10 min for denaturing. Next the solution was compensated to create a final concentration of 1% Nonidet P-40 and 50 mM Na_2PO_4 prior to the addition of 5 units of PNGase F. This solution was incubated at 37 °C for 2 h prior to subjecting the released glycans in this solution to reductive amination derivatization.

Derivatization. Reductive amination of oligosaccharides and glycans were conducted using a reductive amination procedure previously described by Prime et al.¹⁵ A 10 μ L oligosaccharide solution (LNFP series and LNDFH series) at a concentration of 500 μ M or \sim 10 μ g of released glycans were mixed with a 10 μ L solution of the amine-containing fluorophore (\sim 0.5 M) in 7:3 DMSO/HOAc solution, which was heated for 1 h at 65 °C. Twenty microliters of 1 M $NaCNBH_3$ was added to this solution and heated for another hour at 65 °C. Derivatized oligosaccharides and glycans were desalted and removed from excess fluorophore by porous graphitic carbon CarboGraph Extract-Clean SPE columns

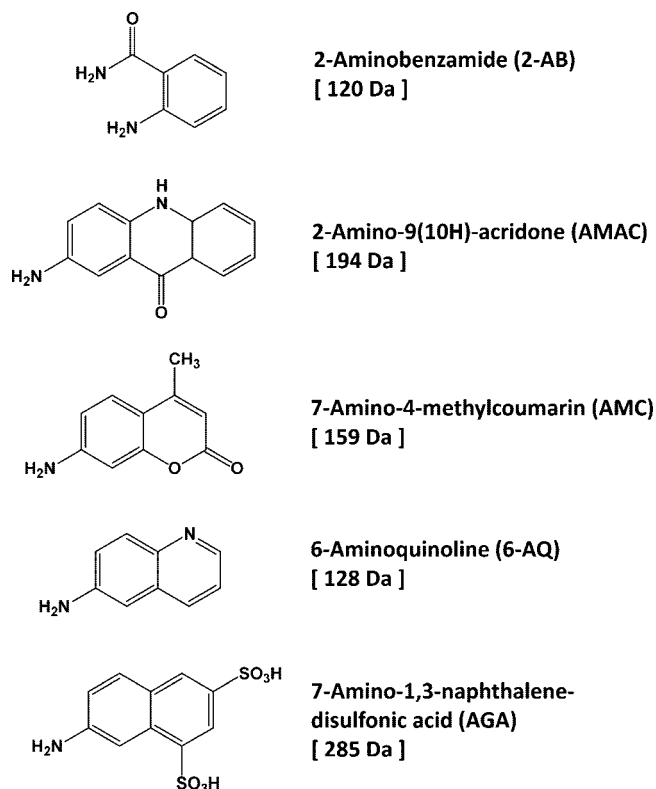


Figure 1. Structures of the fluorescent reagents for reductive amination of oligosaccharides. In parentheses next to the name is the chemical abbreviation. The nominal mass addition to the oligosaccharide is included in brackets.

(Alltech Associates, Inc., Deerfield, IL) following the protocols described by Packer et al.⁵⁹

Mass Spectrometry. A ThermoFinnigan LCQ Deca XP (San Jose, CA) modified for UVPD, was employed for all mass spectrometry experiments as further described in the next section.⁵⁵ Analyte solutions were diluted to a concentration of 10 μM in a 50/50 ACN/H₂O (v/v) solvent mixture for ESI-MS analysis. These solutions were infused into the mass spectrometer at a flow rate of 3–5 $\mu\text{L}/\text{min}$ with a Harvard Apparatus PHD 2000 syringe pump (Holliston, MA). Ion activation by CID was conducted at the default q_z values of 0.25 and 30 ms. The CID and UVPD MS/MS spectra were characterized with the aid of the web application GlycoFragment.⁶⁰

Ultraviolet Photodissociation. UVPD experiments were performed on an LCQ Deca instrument previously described in full detail.⁵⁵ In brief, this mass spectrometer was equipped with an unfocused Quanta-Ray GCR-11 Nd:YAG laser with a HG-2 harmonics generator from Spectra-Physics (Mountain View, CA) for the creation of 355 nm photons. A CF viewport was incorporated into the top vacuum flange mount for transmission of the UV photons through an antireflective quartz window from CVI laser (Albuquerque, NM). The Nd:YAG laser was gated by a TTL signal output from the instrument, which was controlled by the instrument software. This TTL signal was increased to 15 V through an operational amplifier circuit integrated into the laser

control unit for triggering the laser. The laser was operated at 10 Hz with full energy pulses at (~ 60 mJ/pulse) with the number of pulses reported unless otherwise noted.

RESULTS AND DISCUSSION

This comparative study of CID and UVPD methods applied to fluorescently labeled oligosaccharides was conducted to evaluate the diagnostic value of the resulting MS/MS spectra for determination of the branching structures. A previous study by our group reported the utility of 355 nm UVPD applied to chromophore-derivatized peptides in which several distinct advantages over traditional CID methods were highlighted.⁵⁵ Among these advantages, the secondary dissociation of chromophore-containing fragment ions upon UV irradiation was particularly valuable for providing a greater array of diagnostic sequence ions. Oligosaccharides, much like other biopolymers, do not readily absorb photons over large regions of the UV–visible light spectrum and therefore must be modified to undergo efficient photodissociation at 355 nm. However, unlike proteins and nucleic acids, oligosaccharides are far more difficult to analyze by conventional spectroscopic methods, a factor that has led to the frequent utilization of derivatization strategies to improve detection limits.¹⁴ The incorporation of amine-containing fluorophores, one common approach, also makes the oligosaccharides amenable to UVPD mass spectrometry. Fluorophores appended to oligosaccharides by reductive amination include 2-AB, AMAC, AMC, 6-AQ, and AGA (see Figure 1), all of which promote UV absorption at $\lambda_{\text{ex}} \sim 355$ nm. These amine-containing reagents selectively react with the anomeric carbon located on the reducing end of the oligosaccharide, which restricts the derivatization of these analytes to one specific site at the core of the structure. The reaction proceeds through a Schiff base intermediate, which is then reduced to form a stable linkage between the reducing end sugar and the appended fluorophore as depicted in Scheme 1.

MS/MS Characterization of the LNFP Oligosaccharide Series. The elucidation of branching structures of isomeric oligosaccharides has been accomplished previously by tandem mass spectrometry. For example, CID of sodium-cationized oligosaccharides typically yields fragment ions containing the reducing end sugar. As an example, the CID mass spectra of sodium-cationized LNFP-I, -II, -III, and -V are shown as Supporting Information (Figure S1) for benchmark purposes. The chemical and symbolic structures of these oligosaccharides are shown in Figure 2 for comparison. After derivatization with the fluorophore 6-AQ, the LNFP oligosaccharides also produce reducing end fragments upon CID (Figure 3). All mass spectra in this study are labeled with arrows to indicate possible sugar losses (which do not necessarily imply specific fragmentation pathways) as well as accepted oligosaccharide fragmentation nomenclature (A, B, C, Y) ions.²¹ In Figure 3, partial differentiation of the LNFP-I, -II, and -III isomers from the LNFP-V isomer is possible based on the presence of the B₂ fragment ion in the CID mass spectra of the former and the ^{0,3}A₄ ion in the CID mass spectrum of the latter. The diagnostic fragment ions that specifically allow isomer differentiation are labeled with an inverted triangle (∇) symbol in the mass spectra for easy recognition throughout this study. Unfortunately, these CID mass spectra are not sufficiently unique to allow successful differentiation of the first three LNFP isomers.

(59) Packer, N. H.; Lawson, M. A.; Jardine, D. R.; Redmond, J. W. *Glycoconjugate J.* **1998**, *15*, 737–747.

(60) Lohmann, K. K.; Von Der Lieth, C.-W. *Nucleic Acids Res.* **2004**, *32*, W261–W266.

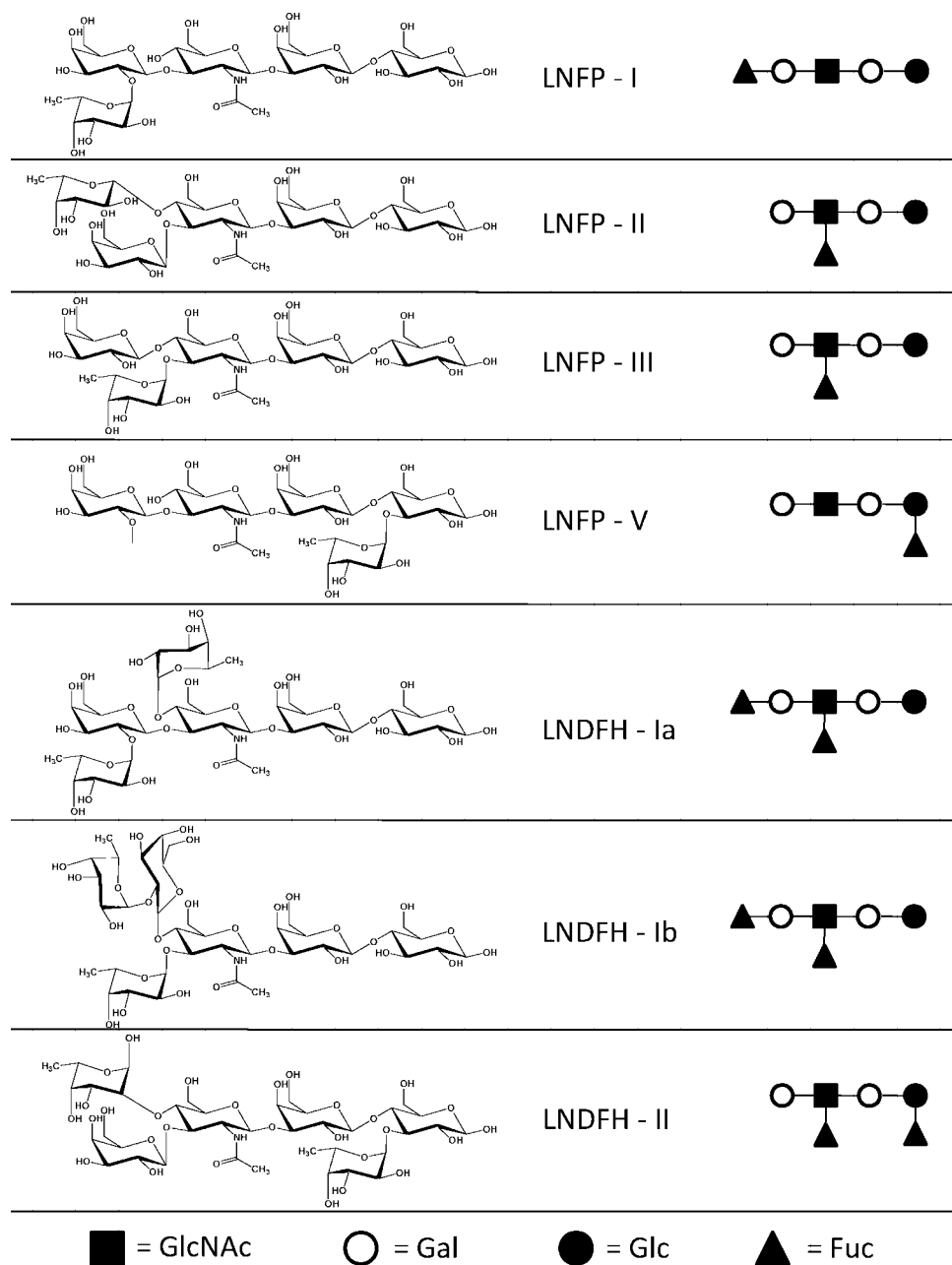


Figure 2. Chemical and symbolic structures of the LNFP oligosaccharide series and the LNDFH oligosaccharide series.

The corresponding UVPD mass spectra for the same four isomeric fluorophore-derivatized, sodium-cationized oligosaccharides display vastly different information from the CID mass spectra, as shown in Figure 4. The most notable difference is that the detected fragment ions stem from the nonreducing end of the oligosaccharide, which primarily yields A- and C-type ions, as opposed to the dominant Y-type ions produced upon CID. Another common feature of the UVPD spectra is the loss of the fluorophore group in conjunction with part of the reducing sugar, and these characteristic losses are labeled as -6-AQ^* and $-6\text{-AQ}''$, corresponding to formation of $^{0,1}\text{A}$ - and $^{0,2}\text{A}$ -type fragment ions, respectively. These types of fragments are illustrated in the bottom structure of Scheme 2. The complementary loss of the remaining reducing end monomeric sugar moiety via cleavage of the glycosidic bond is labeled as $-\text{Glc}^*$. In general, the UVPD mass spectra show more unique

fragments than the CID mass spectra, thus enhancing isomer differentiation of the LNFP oligosaccharides. For example, the additional loss of the fructose group ($-\text{Fuc}$) from the $^{0,2}\text{A}_5$ fragment is observed only for the LNFP-I isomer in the UVPD mass spectrum (Figure 4A). Additionally, new fragment ions such as the C_2 and $\text{C}_2/\text{Y}_{3\alpha}$ ions can be utilized for differentiation of LNFP-II and -III from the LNFP-V isomers. However, the LNFP-II and -III isomers remain indistinguishable from one another even upon UVPD, presumably due to the similarities in their structures, differing only by their Fuc linkage to GlcNAc ($\alpha 1-3$ vs $\alpha 1-4$), which requires highly specific cross-ring cleavages at this position for identification. Similar results as those highlighted in Figures 3 and 4 are obtained when the other fluorophores are attached to these four oligosaccharides. These results are promising in that CID and UVPD provide complementary MS/MS information by affording sequence ions

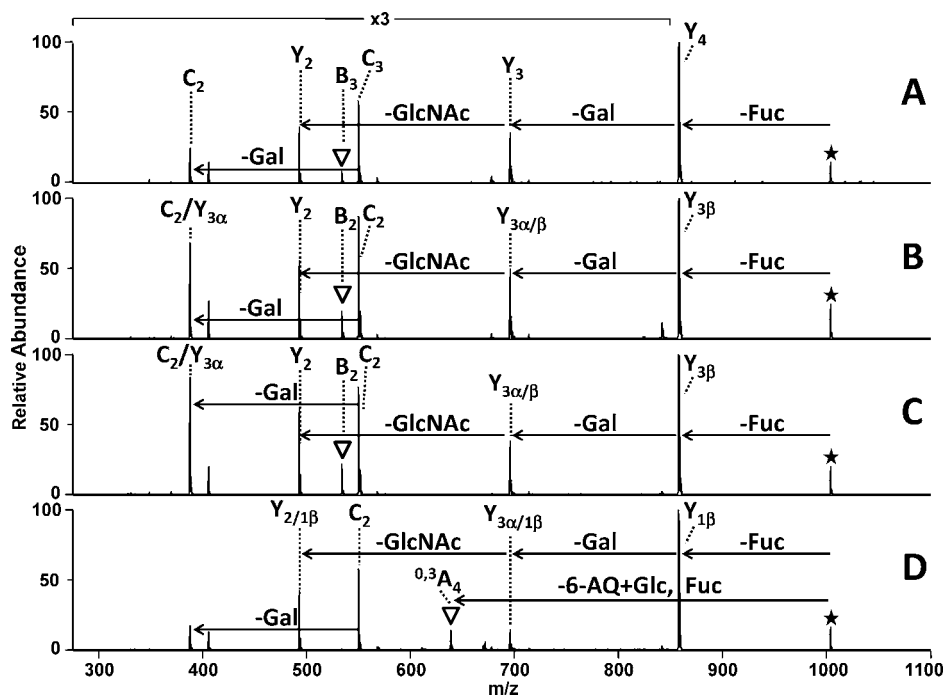


Figure 3. ESI-MS/MS spectra of (A) [LNFP-I + Na + 6-AQ]⁺, (B) [LNFP-II + Na + 6-AQ]⁺, (C) [LNFP-III + Na + 6-AQ]⁺, and (D) [LNFP-V + Na + 6-AQ]⁺ by CID. The triangle symbol (▽) represents unique fragments useful in isomeric differentiation. Loss of the fluorophore reagent and reducing sugar glucose is labeled –6-AQ+Glc. A star symbol (★) is used to signify the precursor ion. The magnification scale bar applies to all spectra over the indicated mass range.

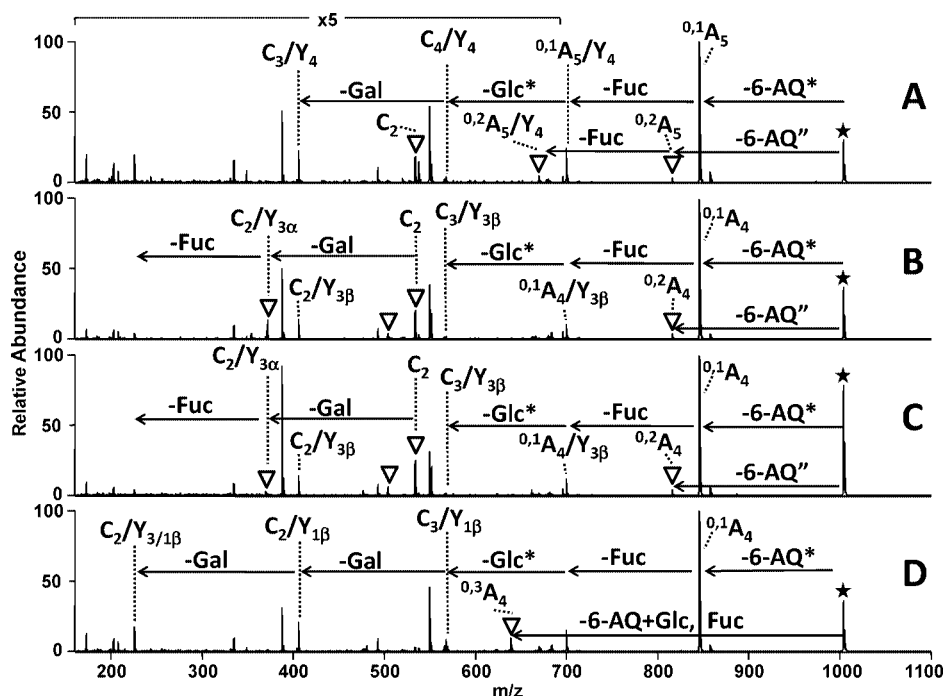


Figure 4. ESI-MS/MS spectra of (A) [LNFP-I + Na + 6-AQ]⁺, (B) [LNFP-II + Na + 6-AQ]⁺, (C) [LNFP-III + Na + 6-AQ]⁺, and (D) [LNFP-V + Na + 6-AQ]⁺ by UVPD using 20 pulses at 60 mJ/pulse for all four spectra. The triangle symbol (▽) represents unique fragments useful in isomeric differentiation. Loss of the fluorophore reagent by cross-ring cleavage of the reducing sugar is labeled –6-AQ* and –6-AQ'', representing formation of ^{0,1}A- and ^{0,2}A-type fragment ions, respectively. Loss of the fluorophore reagent and reducing sugar glucose is labeled –6-AQ+Glc. A star symbol (★) is used to signify the precursor ion. The magnification scale bar applies to all spectra over the indicated mass range.

from opposite ends of the oligosaccharides, a particularly desirable outcome for analysis of complex, nonlinear biopolymers.

MS/MS Characterization of the LNDFH Oligosaccharide Series. The same features noted in the UVPD and CID mass spectra of the fluorescently labeled LNFP series are relevant for

the differentiation of a more complex series of oligosaccharides, namely the LNDFH series. The CID mass spectra of the sodium-cationized LNDFH isomers are displayed in the Supporting Information section (Figure S2). For comparative purposes, a second fluorophore reagent, AMC, was used instead of 6-AQ to

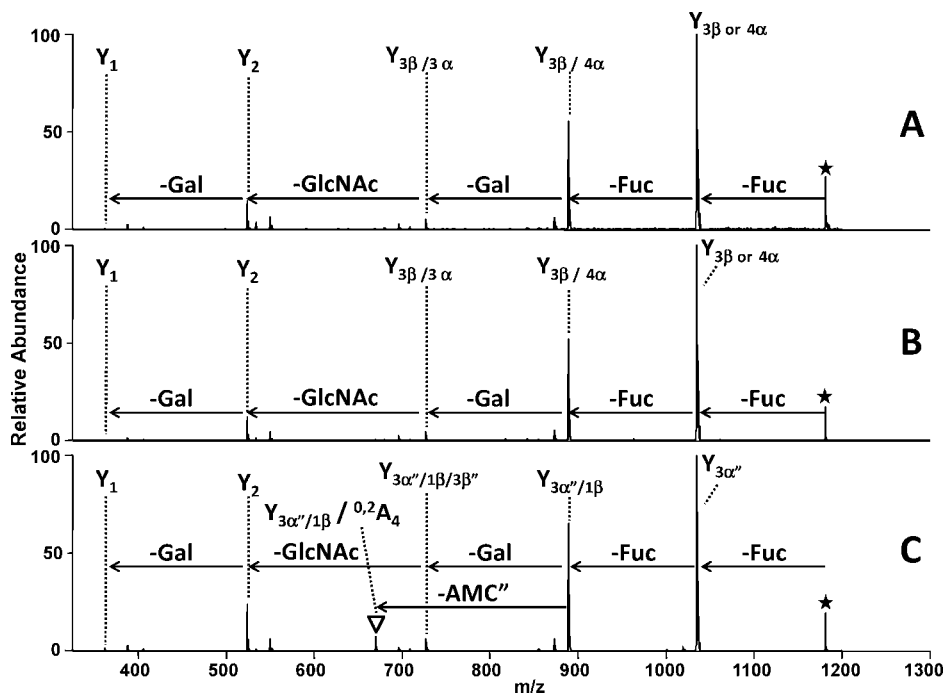


Figure 5. ESI-MS/MS spectra of (A) [LNDFH-Ia + Na + AMC]⁺, (B) [LNDFH-Ib + Na + AMC]⁺, and (C) [LNDFH-II + Na + AMC]⁺ by CID. The triangle symbol (▽) represents unique fragments useful in isomeric differentiation. Loss of the fluorophore reagent by cross-ring cleavage of the reducing sugar is labeled -AMC'', yielding the ^{0,2}A-type fragment ion. A star symbol (★) is used to signify the precursor ion.

derivatize this series of compounds. The resulting CID and UVPD mass spectra for the sodium-cationized fluorophore-labeled oligosaccharides are shown in Figures 5 and 6, respectively. The chemical and symbolic structures of these LNDFH oligosaccharides are shown in Figure 2. The CID mass spectra obtained for the LNDFH-Ia and LNDFH-Ib complexes, Figure 5A and B, respectively, reveal similar fragmentation patterns, which is typical for isomers differing only in their Fuc-GlcNAc linkage, in this case α 1-3 versus α 1-4. The CID mass spectrum for the third isomer, LNDFH-II (Figure 5C), reveals one new fragment ion attributed to the loss of the fluorophore from the reducing sugar (^{0,2}A₄/Y_{3 α '/1 β , labeled ▽) that could differentiate this isomer; however, the abundance of this single unique fragment ion is low, thus limiting the confidence in identifying this oligosaccharide.}

The corresponding UVPD mass spectra for these AMC-labeled LNDFH oligosaccharides display notably different fragmentation patterns as shown in Figure 6. Again the major fragment ions do not contain the fluorophore and stem from the nonreducing end of the oligosaccharide, yielding A- and C-type ions as opposed to the Y-type ions created by CID. Cross-ring cleavages of the reducing sugar containing the fluorophore that occur for the LNDFH isomers result in the formation of two highly diagnostic ions, ^{0,2}A₅ for LNDFH-Ia and LNDFH-Ib and ^{0,1}A₄/Y_{3 α ' for LNDFH-II, that allow differentiation of LNDFH-II from the Ia and Ib isomers. Moreover, another series of fragment ions (labeled ▽, C_{3 α} ions) permit differentiation of the LNDFH-Ia and -Ib isomers from LNDFH-II. For example, the C₄ ion can be used to distinguish LNDFH-Ia and -Ib from LNDFH-II, whereas the C_{3 α} and C_{3 α '/Y_{3 β '} ions are useful for discrimination of LNDFH-II from -Ia and -Ib.}}

A summary of the two main categories of ions produced upon CID and UVPD of [AMC-LNDFH-II + Na]⁺ is shown in Figure

7. The CID collision activation voltage (which influences the ion collision energies and internal energy deposition) or the number of UV laser pulses (which corresponds to total energy deposition) was varied while monitoring the total abundances of all reducing end fragment ions containing the fluorophore and all nonreducing end fragment ions compared to the abundance of the precursor ions (based on peak areas). Figure 7A displays the energy-variable CID fragmentation trends, which show a striking dominance of reducing end fragments containing the fluorophore as the CID voltage is raised. A small portion of nonreducing end fragment ions are observed but remain less than 5% throughout the range of CID collision energies. In contrast, the UVPD data acquired as a function of the number of laser pulses for this same AMC-derivatized oligosaccharide indicate that the nonreducing end fragment ions are dominant with the fluorophore-containing reducing end fragments representing less than 5% of the total abundance (Figure 7B). Interestingly, the pulse-variable UVPD shows a significant abundance of reducing end fragment ions from one to three pulses, which indicates that these ions are formed but decompose upon exposure to subsequent laser pulses. In fact, the single-pulse UVPD spectrum actually affords a 4:1 ratio of reducing end to nonreducing end fragment ions, albeit at low total abundance, which is similar to the distribution observed from the CID data in which the reducing end fragment ions are consistently more dominant. In contrast, multiple-pulse UVPD produces more nonreducing fragment ions, which is attributed to the efficient secondary dissociation of all fluorophore-containing fragments (i.e., the reducing end fragments), which are capable of further photon absorption and dissociation upon subsequent laser pulses during UV activation. The secondary dissociation of the primary fluorophore-containing fragment ions in turn creates a combination of observed internal fragment ions and nonreducing end fragment

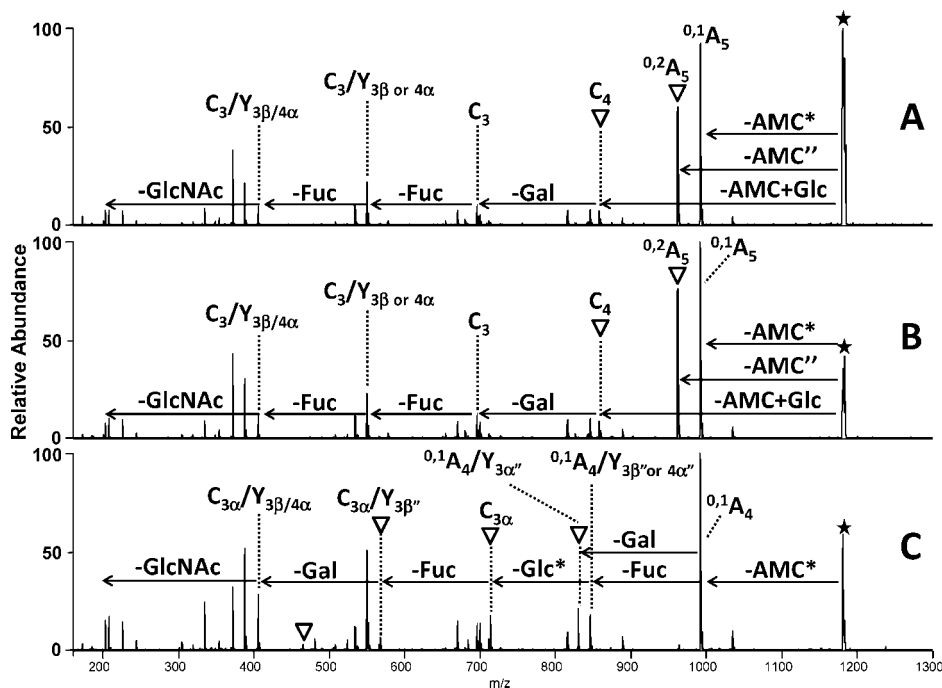


Figure 6. ESI-MS/MS spectra of (A) $[\text{LNDFH-Ia} + \text{Na} + \text{AMC}]^+$, (B) $[\text{LNDFH-Ib} + \text{Na} + \text{AMC}]^+$, and (C) $[\text{LNDFH-II} + \text{Na} + \text{AMC}]^+$ by UVPD with 20 pulses at 60 mJ/pulse for all three spectra. The triangle symbol (∇) represents unique fragments useful in isomeric differentiation. Loss of the fluorophore reagent by cross-ring cleavage of the reducing sugar is labeled $-\text{AMC}^*$ and $-\text{AMC}''$, resulting in formation of $^{0,1}\text{A}$ - and $^{0,2}\text{A}$ -type fragment ions, respectively. Loss of the fluorophore reagent and reducing sugar glucose is labeled $-\text{AMC}+\text{Glc}$. A star symbol (\star) is used to signify the precursor ion.

ions, as well as fragment ions in the low m/z range that are not detectable. This highly efficient secondary dissociation of the fluorophore-containing reducing end fragment ions upon UVPD ultimately results in the observed MS/MS spectra, which are dominated by nonreducing end fragments and thus complementary to the CID mass spectra.

Influence of Fluorophore on UVPD Efficiency. The ideal fluorophores for oligosaccharide analysis will allow both fluorescence quantification and UVPD characterization, in addition to increasing the hydrophobicity of the targeted oligosaccharides for improved separation by HPLC.⁶¹ For MS/MS identification by UVPD, the fluorophore should not only undergo efficient photon absorption but also promote diagnostic dissociation of the oligosaccharides, as opposed to less meaningful pathways such as cleavage of the fluorophore tag. Therefore, the relative PD efficiency afforded by incorporation of different fluorophore labels is a key performance parameter. Absorption and fluorescence properties of fluorophore-labeled oligosaccharides in solution may differ dramatically from the analogous data for gas-phase ions due to the impact of solvation and charge state, and thus, UVPD dissociation efficiencies are best predicted from energy-variable UVPD measurements in the gas phase. For these experiments, the relative extent of UVPD is measured for an oligosaccharide as a function of the fluorophore tag for a fixed set of UVPD parameters (e.g., 20 laser pulses at 60 mJ/pulse). Examples of the resulting comparative UVPD spectra are shown in Figure 8 for LNDFH-Ia derivatized with four different fluorophores. Figure 8A shows the UVPD spectrum obtained for protonated 6-AQ-LNDFH-Ia,

and panels B–E in Figure 8 show the UVPD spectra obtained from the precursor $[\text{LNDFH-Ia} + \text{Na} + \text{fluorophore}]^+$ for fluorophores 6-AQ, 2-AB, AMAC, and AMC, respectively. Different degrees of magnification were applied to each spectrum to emphasize the similarities in the resulting fragmentation pathways irrespective of the fluorophore. As noted in earlier sections, the fragment ions produced upon UVPD mainly stem from neutral losses that incorporate the fluorophore tag. Based on the specific fluorophore tag, the relative UVPD efficiencies of the LNDFH-Ia ions are summarized in decreasing order as follows: 6-AQ $[\text{Na}^+]$ (65.0%); AMAC (48.6%); AMC (41.9%); 6-AQ $[\text{H}^+]$ (21.0%); and 2-AB (10.5%). A similar trend is observed for other fluorophore-labeled oligosaccharides, and these data support 6-AQ as the best reagent for UVPD strategies.

Figure 8A shows the UVPD spectrum of protonated 6-AQ-LNDFH-Ia for comparison to that of sodium-cationized 6-AQ-LNDFH-Ia (Figure 8B). The UVPD spectra of protonated oligosaccharides actually afford rather convoluted branching structure information due to fructose rearrangements, which have previously been observed upon collision-induced dissociation of protonated reductively aminated oligosaccharides.⁶² Franz et al. proposed a two-step proton-catalyzed mechanism that facilitates a long-range glycosyl-transfer reaction for protonated oligosaccharides that are fluorescently labeled.⁶² This feature makes structural elucidation of protonated oligosaccharides difficult, but fortunately, the sodium-cationized species follow predictable fragmentation routes and thus are preferred for MS/MS applications. Moreover, the difference in UVPD efficiencies for the

(61) Delaney, J.; Vouros, P. *Rapid Commun. Mass Spectrom.* **2001**, *15*, 325–334.

(62) Franz Andreas, H.; Lebrilla Carlito, B. *J. Am. Soc. Mass Spectrom.* **2002**, *13*, 325–337.

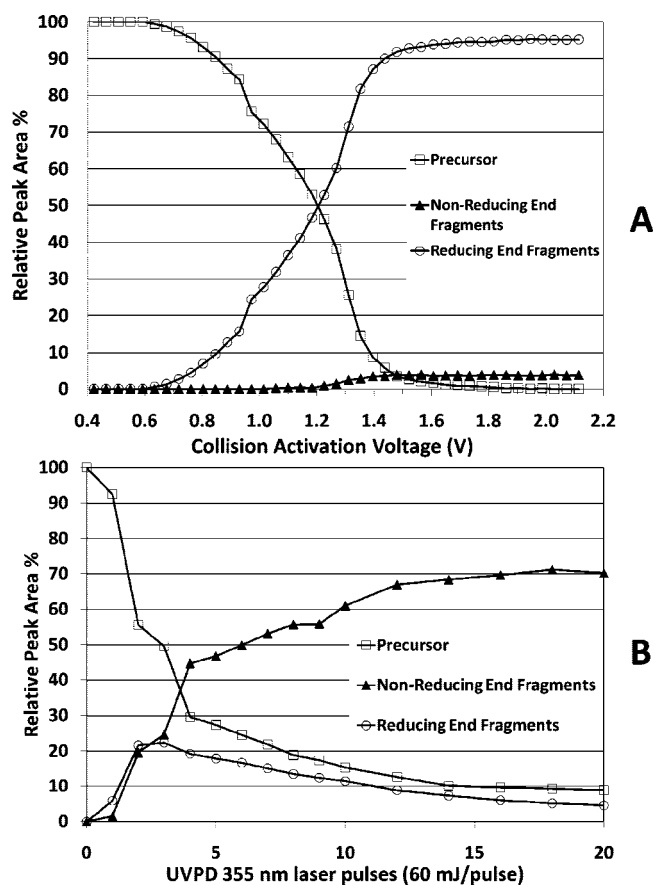


Figure 7. Relative peak area abundance of the precursor, sum of nonreducing end fragments, and sum of reducing end fragments versus (A) CID collision activation voltage and (B) the number of laser pulses (355 nm, 60 mJ/pulse at 10 Hz) of [LNDFH-II + Na + AMC]⁺.

protonated (21%) versus sodium-cationized (65%) LNDHFH-Ia species is significant, which also argues against using the protonated species for UVPD applications.

MS/MS of High-Mannose Glycans Released from Ribonuclease B. Glycans can also be derivatized to undergo efficient UVPD after their enzymatic release from glycoproteins and subsequent reductive amination. Ribonuclease B is a good model protein due to its relatively simple glycan composition that incorporates five variants of the high-mannose N-linked glycan (GlcNAc₂Man₅₋₉). These glycans were released from the glycoprotein by enzymatic treatment with PNGase F and then derivatized with 6-AQ. The two most abundant of these glycans, GlcNAc₂Man₅ and GlcNAc₂Man₆, were subjected to CID and UVPD with the resulting MS/MS spectra shown in Figure 9. Interestingly, unlike the LNFP and LNDFH oligosaccharides, these glycans have a tendency to lose the fluorophore upon activation, yielding B-type fragment ions by CID (Figure 9A and C). Consequently, these CID spectra afford information more similar to their UVPD counterparts (Figure 9B and D) than noted for the earlier CID versus UVPD comparisons for the oligosaccharides; however, there are still several distinct differences. In contrast to the CID mass spectra, the UVPD spectra display not only ^{0,1}A- and ^{0,2}A-type fragment ions but also dominant C-type ions that were not observed in the corresponding CID spectra, as opposed to the more prevalent B-type fragment ions seen in the CID mass spectra. The prevalent formation of C-type ions

instead of B-type ions upon UV irradiation is suggestive of greater internal energy deposition than that which occurs during collisional activation and is supported by the fact that C-type fragment ion formation is more commonly observed in high-energy CID experiments.²² Based on this observation, it is probable that the labeled (Man)₃₋₅ fragment ions in the UVPD spectra could be the result of glycosidic bond cleavages that lead to C-/Z-ions instead of B-/Y-ions, which result in isomeric fragment overlap. For example, in Figure 9B, “B₃/Y_{3β} or 4_α” could in fact be created from “C₃/Z_{3β} or 4_α”, in both cases resulting in ions containing four mannose units (Man)₄. Due to this uncertainty in identification, many of these fragments are simply labeled (Man)_x where *x* is the number of remaining mannose units. This data demonstrates the potential for characterization of glycans released from glycoproteins by implementing UVPD to probe key diagnostic fragment ions.

Fluorophore-Assisted Electron Photodetachment Dissociation. The attachment of fluorophores to oligosaccharides also offers the option of pursuing electron photodetachment dissociation⁴² strategies instead of UVPD. In EPD, negatively charged ions undergo electron detachment upon laser irradiation to produce charge-reduced radical ions. The charge-reduced radical ions may exhibit different dissociation routes upon subsequent collisional activation than conventional closed-shell anions. For oligosaccharides, EDD, a method in which deprotonated molecules stored in an FTICR mass spectrometer are irradiated with electrons, thus causing electron detachment and ion dissociation, results in additional cross-ring cleavages such as ^{3,5}A-, ^{1,5}A-, ^{1,5}X-, and ^{3,5}X-type ions, which can greatly assist in linkage characterization.²⁹ In contrast to EDD, EPD has not been previously reported for the analysis of oligosaccharides, in large part because underivatized oligosaccharides do not efficiently absorb UV photons. For the present work, an acidic fluorophore was used to derivatize the oligosaccharides in order to ensure the efficient formation of doubly charged negative ions upon ESI. Examples of the resulting EP and EPD spectra are shown in Figure 10 for LNDFH-II derivatized with AGA. Figure 10A shows the electron photodetachment spectrum obtained upon UV irradiation of the doubly deprotonated precursor, resulting in conversion of [(M + AGA) - 2H]²⁻ ions to charge-reduced [(M + AGA) - 2H]⁻ radical species. Confirmation that the charge-reduced products formed upon the UV irradiation are in fact radical species is obtained by expansion of the molecular ion region and comparison to the molecular ion region of conventional deprotonated LNDFH-II (Figure 10D). The radical species appears 1 Da lower in mass than the conventional deprotonated species, which is consistent with its origins from a doubly deprotonated precursor. When the [(M + AGA) - 2H]⁻ radical ion is subsequently subjected to CID, the EPD spectrum in Figure 10B is obtained. The fragmentation pattern of the radical ion is dramatically different from that of the conventional singly deprotonated precursor (Figure 10C). The CID spectrum of the conventional deprotonated oligosaccharide in Figure 10C displays mainly Y-type fragment ions, whereas the EPD spectrum in Figure 10B reveals Y-, Z-, and cross-ring cleavage X-type fragment ions. These striking differences in the fragmentation patterns of the radical ions and deprotonated species

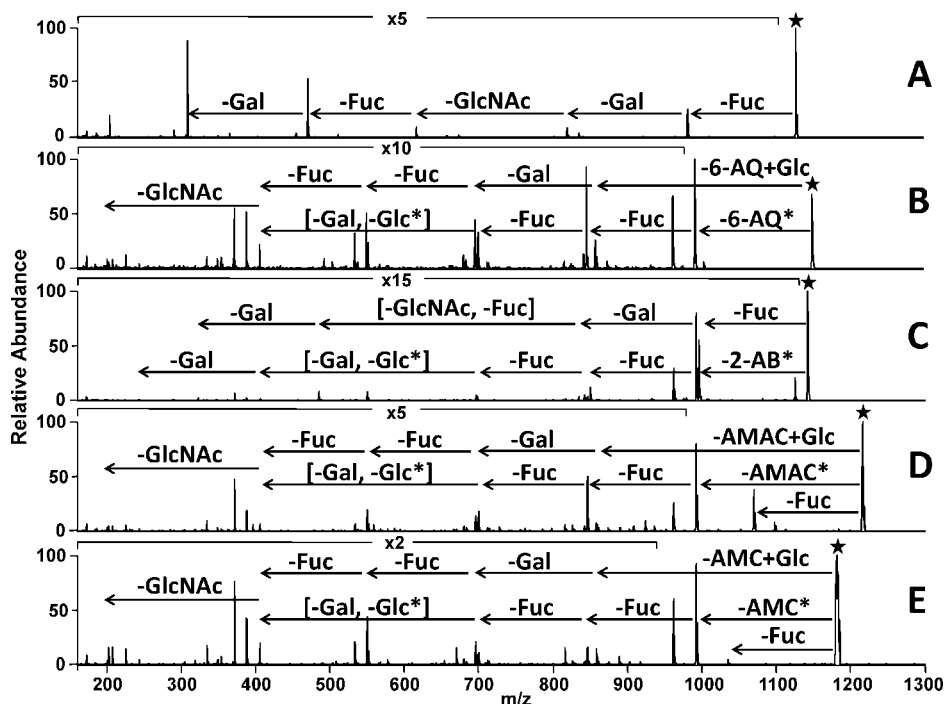


Figure 8. ESI-MS/MS of $[LNDFH-Ia + Na + \text{label}]^+$ comparing the relative dissociation efficiencies of different fluorescent labels in parentheses including (A) 6-AQ $[H^+]$ (21.0%), (B) 6-AQ $[Na^+]$ (65.0%), (C) 2-AB (10.5%), (D) AMAC (48.6%), and (E) AMC (41.9%) by UVPD using 20 pulses for all five spectra. A star symbol (★) is used to signify the precursor ion. Loss of the fluorophore reagent by cross-ring cleavage of the reducing sugar is labeled $-FL^*$ and $-FL''$ (where FL is a generic term used to represent 6-AQ, AMAC, AMC, or 2-AB), resulting in formation of $^{0,1}A$ - and $^{0,2}A$ -type fragment ions, respectively. Loss of the fluorophore reagent and reducing sugar glucose is labeled $-FL+Glc$. Various degrees of magnification are shown for each spectrum over the indicated mass range to scale up the fragment ions to allow easier visual comparison.

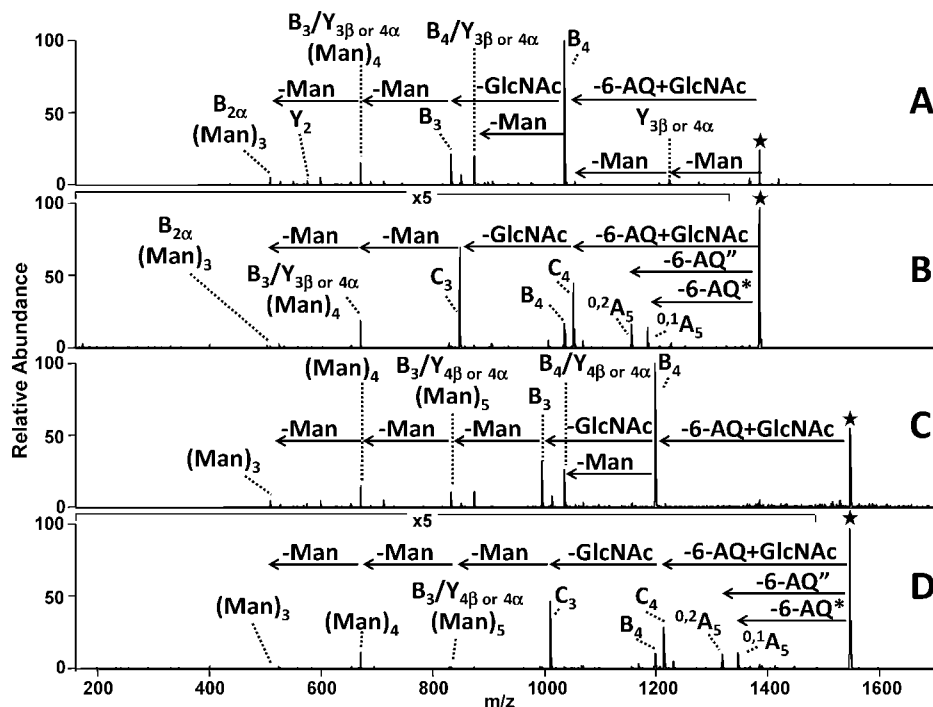


Figure 9. ESI-MS/MS spectra of $[GlcNAc_2Man_5 + Na + 6-AQ]^+$ by (A) CID and (B) UVPD with 20 pulses and $[GlcNAc_2Man_6 + Na + 6-AQ]^+$ by (C) CID and (D) UVPD with 20 pulses. A star symbol (★) is used to signify the precursor ion. Loss of the fluorophore reagent by cross-ring cleavage of the reducing sugar is labeled $-6-AQ^*$ and $-6-AQ''$, resulting in formation of $^{0,1}A$ - and $^{0,2}A$ -type fragment ions, respectively. Loss of the fluorophore reagent and reducing sugar is labeled $-6-AQ+GlcNAc$. The magnification scale bars apply only to (B) and (D) over the indicated mass range.

are under further investigation and may lead to development of EPD as a promising tandem mass spectrometric method for

characterization of oligosaccharides. Derivatization of the oligosaccharides with the nonacidic fluorophores shown in

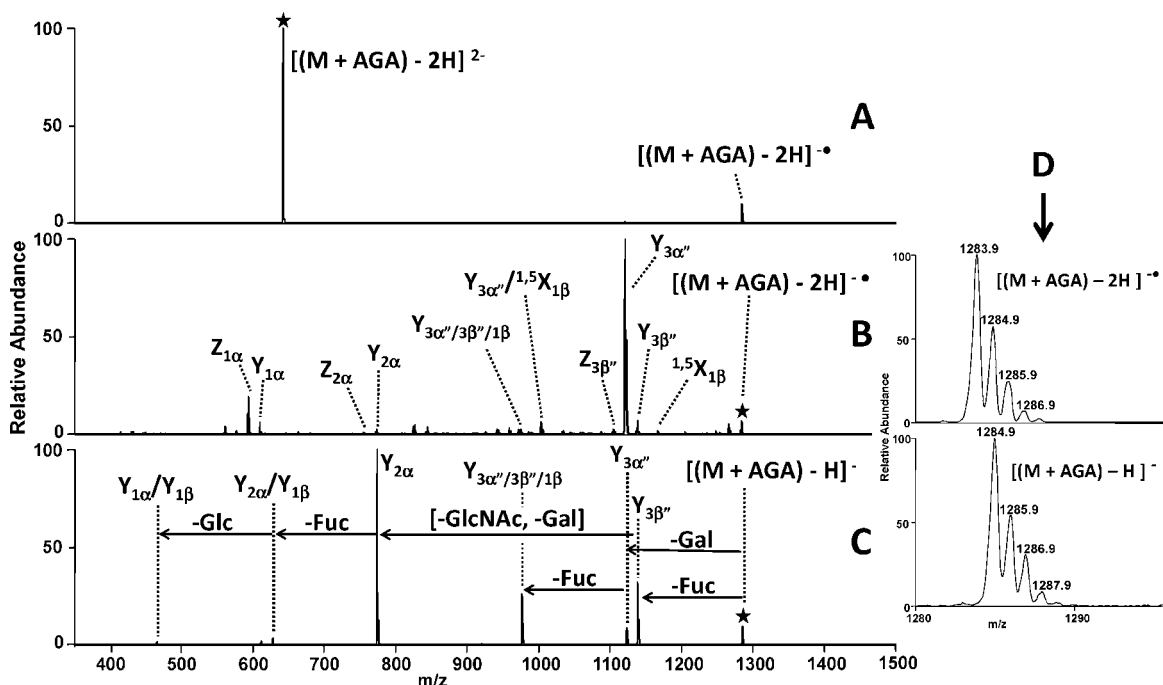


Figure 10. Electron photodetachment dissociation of LNDFH-II derivatized with AGA, where (A) shows the EPD spectrum upon irradiation of doubly deprotonated LNDFH-II using 20 laser pulses resulting in production of the radical species $[M + \text{AGA} - 2\text{H}]^{\cdot-}$. (B) CID of the resulting radical ion; (C) CID of $[\text{LNDFH-II} + \text{AGA} - \text{H}]^-$. (D) Expanded regions around the precursor ions show the 1-Da mass difference between the radical ion and conventional closed-shell deprotonated species. A star symbol (\star) is used to signify the precursor ion.

Figure 1 did not lead to efficient production of negative ions in the negative ESI mode, nor to successful EPD.

CONCLUSION

Fluorescently labeled oligosaccharides undergo efficient UVPD at 355 nm, which leads to production of a complementary series of fragment ions compared to CID. Multiple-pulse UVPD results in extensive secondary dissociation and primarily formation of fragment ions from the nonreducing end in contrast to CID, which typically results in reducing-end fragment ions that retain the appended fluorophore. UVPD shows promise for facile isomeric differentiation of oligosaccharides, especially in combination with CID experiments for comprehensive structural characterization. This method has been extended to a model glycoprotein, ribonuclease B, based on enzymatic release of the glycans, subsequent derivatization, and UVPD analysis. The first EPD results for fluorophore-derivatized oligosaccharides showcase cross-ring cleav-

ages not typically observed for conventional closed-shell deprotonated species nor sodium-cationized complexes.

ACKNOWLEDGMENT

Funding from the Welch Foundation (F1155), the National Science Foundation (CHE-0718320) and an NSF/IGERT fellowship to J.J.W. (D6E-03333080) are gratefully acknowledged.

SUPPORTING INFORMATION AVAILABLE

Additional information as noted in text includes two supplemental figures: CID MS/MS spectra of sodium-cationized LNFP-I, -II, -III, and -V, as well as LNDFH-Ia, -Ib, and -II. This material is available free of charge via the Internet at <http://pubs.acs.org>.

Received for review February 14, 2008. Accepted April 10, 2008.

AC800315K